chemical reagents of P_2O_5, $ZnSO_4$, MgO and Ho_2O_3 (Sigma Aldrich, 99% purity) in powder (as raw materials) form were taken as glass constituents. A batch of homogeneously ground mixture of 22 g were placed in an alumina crucible and then preheated for 30 minutes before being melted in an electrical furnase at 1100℃ for 1.5 hour. The mixture is then annealed at 300℃ for 3 hour and gradually cooled down to room temperature. The frozen solid was cut and polished for optical measurement. Table 1 enlists the compositional designations (MZSPGHx) of the prepared glass system for varying Ho_2O_3 contents of x = 0.0, 0.5, 1.0, 1.5 2.0, and 2.5 mol%.

The glass density was determined using Archimedes method with toluene as immersion liquid. The glass density (ρ) was calculated via:

$$\rho = \frac{W_a}{W_a - W_l}(\rho_l - \rho_a) \tag{1}$$

where W_a and W_l are the weights of the sample in air and in toluene having density ρ_l, and ρ_a is the air density.

The molar volume (V_m) in terms of molecular weight yields:

$$V_M = \frac{M}{\rho} \tag{2}$$

The value of refractive glass index (n) in terms of optical band gap (E_g) was evaluated using (Mahraz et al., 2014):

$$\frac{n^2 - 1}{n^2 + 2} = 1 - \sqrt{\frac{E_g}{20}} \tag{3}$$

The molar refractivity (R_m) and electronic polarizability (χ) was calculated from (Zhao et al., 2007):

$$R_m = \left(\frac{n^2 - 1}{n^2 + 2}\right)V_M \tag{4}$$

$$\chi = \left(\frac{3}{4\pi N}\right)R_m \tag{5}$$

where N is the Avogadro's number.

The room temperature UV-Vis-IR absorption spectra of all prepared samples were recorded using Shimadzu UV-3101PC spectrometer in the wavelength range of 300–1000 nm with a resolution of ±1 nm. The UV edge data of the absorption spectrum was used to evaluate the optical transition and band gap energy. Davis and Mott (Davis and Mott, 1970) formula was exploited to evaluate the optical band gap for the direct and indirect allowed transitions. The optical absorption coefficient, α(ν) was calculated via (Mahraz et al., 2014):

$$\alpha(\nu) = \frac{2.303A}{d} \tag{6}$$

where A is the absorption intensity and d is the sample thickness.

Following standard procedure (Davis and Mott 1970), Tauc plots of all samples were generated to estimate the value of E_g via:

$$\alpha(\nu) = \frac{B(h\nu - E_g)^{1/r}}{h\nu} \tag{7}$$

where B is a constant called band tailing parameter, n is the index number depending on the type of transition and E_g values.

Tauc plot of $(\alpha h\nu)^{1/r}$ versus photon energy ($h\nu$) were drawn by substituting the value of r = ½ in equation (7) for direct allowed transition and r = 2 for indirect allowed transition. Values of direct and indirect E_g were obtained by extrapolating the linear part of $(\alpha h\nu)^2 = 0$ and $(\alpha h\nu)^{1/2}$ curve, respectively

Generally, the band tailing (a measure of defect states or materials disoderness) in the forbidden optical energy band gap that exist in the glass and amorphous materials are characterized in terms of Urbach energy (Jlassi et al., 2016). The Urbach energy (ΔE) of all glass samples was estimated through (Urbach, 1953):

$$\alpha(\nu) = C\exp\left(\frac{h\nu}{\Delta E}\right) \tag{8}$$

where C is a constant.

RESULTS AND DISCUSSION

Physical Properties

Table 1 enlists the values of the density (ρ), molar volume (V_M), refractive index (n), molar refractivity (R_m) and electronic polarizability (χ) of all the the synthesized glass samples.

Table 1 Physical properties of the prepared glass systems.

	MZSPH 0.0	MZSPH 0.5	MZSPH 1.0	MZSPH 1.5	MZSPH 2.0	MZSPH 2.5
ρ (g/cm^3)	2.633	2.675	2.703	2.725	2.754	2.777
V_m (cm^3/ mol)	57.259	56.793	56.638	56.621	56.445	56.396
n	2.200	2.197	2.196	2.194	2.190	2.189
R_m (cm^3)	32.147	31.843	31.736	31.698	31.535	31.489
χ (×10^{-23} cm^3)	1.274	1.262	1.258	1.257	1.250	1.248

Figure 1 shows the Ho_2O_3 concentration dependent variation in the glass density and molar volume. Density being an effective parameter to comprehend the changes in the structure and coordination of glasses (Wu et al., 2016) was evaluated. Glass density was increased with increasing Ho_2O_3 contents which was attributed to the replacement of phosphorous having low molecular weight (141.94 g/mol) by higher molecular weight holmium (377.86 g/mol). Moreover, the larger ionic radii of Ho^{3+} (1.015 Å) that replaced the phosphate (0.17 Å) played a significant role (Shannon, 1976) to make the the glass structure more compact and hence dense. Conversely, the molar volume was reduced from 57.259 to 56.396 cm^3/mol with the addition of Ho_2O_3 which was ascribed to the shrinkage of bond length and inter-atomic distance in the glass network. The glass structure being rich with bridging oxygen (BO) in turn enhanced the network rigidity (Azmi et al., 2015). The declining molar volume is often credited to the improved compactness of the glass network structure (Mhareb et al., 2016).

According to Jlassi (2016), glasses with higher density is most likely to have larger value of refractive index because more ionic

dipoles can be activated in the presence of electric field. However, the refractive index of the current glass system was decreased from 2.200 to 2.189 with increasing Ho_2O_3 contents from 0-2.5 mol%. This reduction in the refractive index values was attributed to the formation of BO because BO are weakly ionic in nature with higher bond energies than non-bridging oxygen (NBO). This resulted a lowering in the electronic polarizability of the studied glass system (El-Mallawany et al., 2013; Singh & Singh, 2014).

The molar refractivity and electronic polarizability was decreased from 32.147 to 31.489 cm^3 and 1.274×10^{-23} to 1.248×10^{-23} cm^3, respectively with increasing Ho_2O_3 concentration. Molar refractivity being a measure of the bonding condition in the glass provided the information about the total drop of the contribution of cationic refraction and oxygen ionic refraction (Mahamuda et al., 2013). The incorporation of Ho_2O_3 indeed led to the structural polymerization and increased the cross-linking in the glass system. Furthermore, low molar refractivity suggested the highly solublity of Ho_2O_3 in the MZSPG system that is required for high lasing transition probabilities, enhanced absorption and stimulated emission cross-section. Electronic polarization together with optical nonlinearity emerges whenever an intense light beam is incident upon a material (Zhao et al., 2007). In the present case, the observed considerable reduction in the electronic polarizability with increasing Ho_2O_3 contents suggested that the cationic charges (Ho^{3+}) seem to hold the cationic electrons (Honma et al., 2000). Moreover, the usual condition where the polarization is directly proportional to field strength is also depends on glass composition (Yusoff & Sahar, 2015). In this regard Ho^{3+} ions probably participated in the glass structure formation, leading towards lowering of the electronic polarizability.

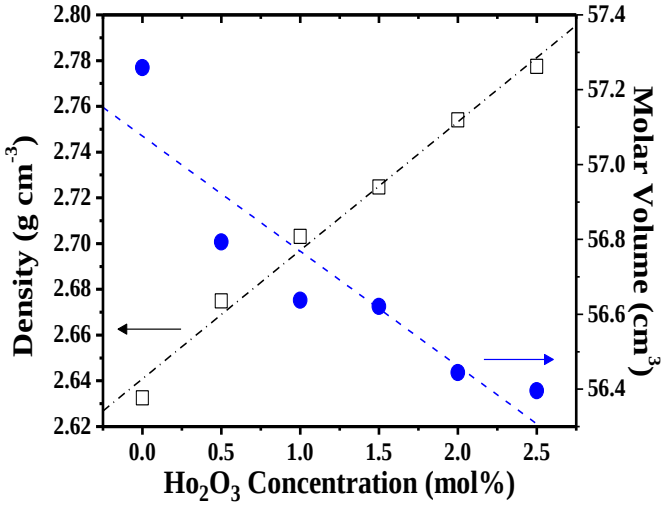

Fig. 1 Ho^{3+} ions content dependent variation in the glass density and molar volume.

Absorption Properties

Figure 2 displays the room temperature UV-Vis absorption spectra of as-synthesized Ho^{3+} doped MZSPG system. It was comprised of nine peaks assigned to the transitions of $^5I_8 \rightarrow {}^3H_6$ (362 nm), $^5I_8 \rightarrow {}^5G_4$ (387 nm), $^5I_8 \rightarrow {}^5G_5$ (418 nm), $^5I_8 \rightarrow {}^5G_6$ (450 nm), $^5I_8 \rightarrow {}^5F_3$ (484 nm), $^5I_8 \rightarrow {}^5F_4 + {}^5S_2$ (538 nm), $^5I_8 \rightarrow {}^5F_5$ (642 nm), $^5I_8 \rightarrow {}^5I_6$ (1148 nm) and $^5I_8 \rightarrow {}^5I_7$ (1945 nm). Occurrences of these absorption bands were attributed to the 4f-4f electronic transitions of Ho^{3+} ions from the ground state ($^5I_8$) to different excited states as indicated. The measured peak positions are consistent with the earlier studies on Ho^{3+} doped barium phosphate (Satyanarayana et al., 2010), fluoro-phosphate (Babu et al. 2015), lead-zinc-borate (Hussain et al., 2006) and tellurite (Seshadri et al., 2014) glass systems. The identification and assignment of the energy levels are in accordance to the existing report (Carnall et al., 1968). Furthermore, the absorption peak appeared sharper and more intense as the Ho_2O_3 concentration was increased. Transition of $^5I_8 \rightarrow {}^3H_6$ and $^5I_8 \rightarrow {}^5G_6$ was identified as hypersensitive because they obeyed the selection rules of $\Delta J \leq 2$, $\Delta L \leq 2$ and $\Delta S = 0$ (Prasad et al., 2003; Seshadri et al., 2014). The pale yellow (~550 nm) color absorption of Ho^{3+} doped glass was overmasked by the strong absorption in the blue violet region (450 nm) (Rai & Fanai 2016).

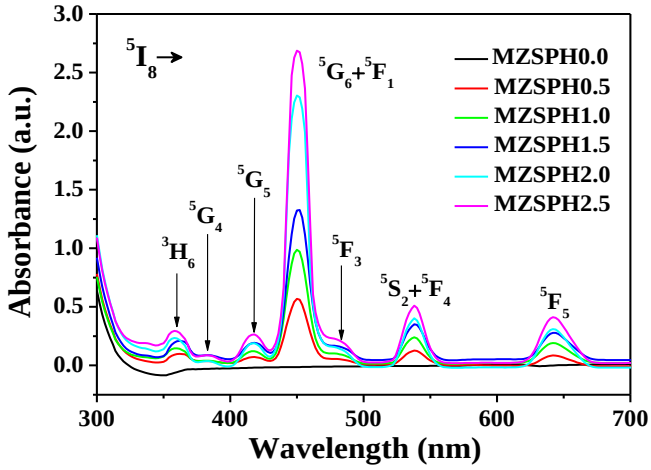

Fig. 2 Absorption spectra of Ho^{3+}-doped MZSPH system.

Further in-depth analysis of the absorption spectra provides useful information about the glass structure and ligand bondings. Full width half maximum (FWHM) of the most intense absorption peak ($^5I_8 \rightarrow {}^5G_6$ at 450 nm) was calculated. Figure 3 illustrates variation of FWHM for the specified peak as a function of Ho_2O_3 contents. The spectral line width of optical transition in REIs doped materials are governed by two major factors. First, the temperature dependent lattice vibration which contributes to the homogeneous line broadening and is common for both amorphous and crystalline materials. Second is the inhomogeneous broadening which is more prominent in non-crystalline material. Inhomogeneous broadening increases the spectral line width and is caused by the site-to-site variation of the ligand field surrounding of REIs (Lee et al., 2008; Mahamuda et al., 2013).

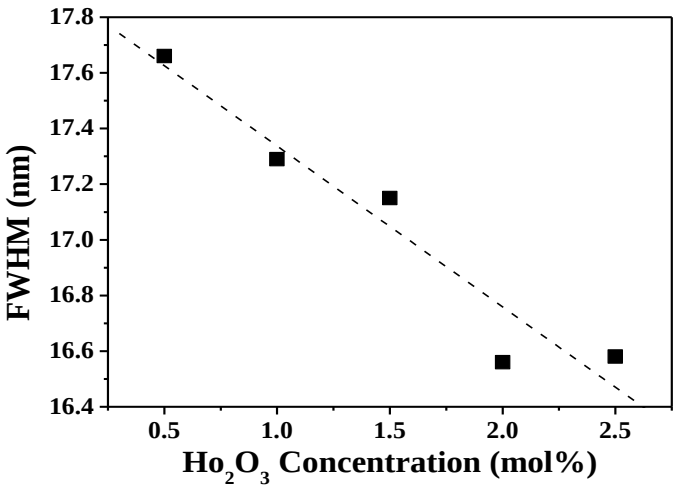

Fig. 3 Ho_2O_3 concentration dependent varition of FWHM for the intense peak appeared at 450 nm.

The observed decrease in the FWHM value from 17.66 to 16.58 nm with the increase of Ho_2O_3 concentration from 0 to 2.5 mol% was attributed to the narrowing of the inhomogeneous broadening (Lee et al., 2008). Actually, the incorporation of Ho_2O_3 might have suppressed the site-to-site interaction in the glass system where the vibronic transitions remains unresolved and hence merged into a broad absorption feature (Alivisatos et al., 1988). Hence, the narrower absorption feature was correlated to the highly well-defined vibronic transitions. The increment of Ho_2O_3 concentration in the glass had shifted the ground and excited electronic potential surface in the vibrational coordinate and led to enhanced line broadening. Table 3 presents the calculated optical band gap and Urbach energy of the synthesized MZSPG system.

Table 3: Optical band gap and Urbach energy of Ho^{3+}-doped MZSPG system

	MZSPH 0.0	MZSPH 0.5	MZSPH 1.0	MZSPH 1.5	MZSPH 2.0	MZSPH 2.5
E_g (eV)	3.847	3.860	3.866	3.875	3.895	3.901
ΔE (eV)	0.257	0.221	0.217	0.271	0.197	0.191

Increase in the optical band gap energy from 3.846 – 3.901 eV with increasing Ho_2O_3 concentration from 0 to 2.5 mol% was attributed to the generation of more BO via the formation of P-O-Ho-O-P chains. The chains linked the phosphate tetrahedral within the glass matrix and enhanced the bond strength. Therefore, BO could bound an electron more tightly than NBO (Khor et al., 2012). In this situation, higher energy was required to excite the electron thereby widening of optical band gap energy of the glass system was observed with increasing Ho_2O_3 concentration. Conversely, the achievement of the low Urbach energy (0.257 to 0.191 eV) of the present glass system with increasing REIs contents indicated the existence of less number of defects/disorder and high compactness of the glass network (Nurhafizah et al., 2016; Yusoff et al., 2015). Reduction of the Urbach energy can be interpretd in terms the generation of local long range order structure in the glass in which increasing concentration of Ho_2O_3 led to the formation of large number of BO and hence enhanced orderness in the structure. This result complemented the enhancement in the optical band gap wherein according to Davis and Mott prediction the presence of high density of localized state in the band structure is responsible for the narrowing of the optical energy band gap (Davis and Mott 1970; Khor et al. 2012).

CONCLUSION

We determined the physical and absorbance characteristics of MZSPH as a function of Ho^{3+} dopding contents. Glass system was prepared via conventional melt-quenching method. Density, molar volume and refractive index were found to vary in the range of 2.633 to 2.777 g/cm^3, 57.259 to 56.396 cm^3/mol and 2.200 to 2.189, respectively. Both molar refractivity and electronic polarizability were reduced with increasing Ho_2O_3 contents. The optical band gap energy (3.847 to 3.901 eV) as well as the Urbach energy (0.257 to 0.191 eV) was strongly influenced by the variation of Eu_2O_3 concentration. The formation of more number of BO was responsible for the alteration of glass network structures. The proposed glass compositions be potential for up/down-converted lasing system.

ACKNOWLEDGEMENT

This work was financially supported by the Universiti Teknologi Malaysia under the Research University Grant and Ministry of Higher Education Malaysia via vote 12H42 (GUP) and 13H50 (GUP).

REFERENCES

Ahmadi, F., R. Hussin, and S. K. Ghoshal. 2016. "Optical transitions in Dy^{3+}-doped magnesium zinc sulfophosphate glass." *Journal of Non-Crystalline Solids* 452:266–72.

Alivisatos, A. P., A. L. Harris, N. J. Levinos, M. L. Steigerwald, and L. E. Brus. 1988. "Electronic states of semiconductor clusters: Homogeneous and Inhomogeneous Broadening of the Optical Spectrum." *The Journal of Chemical Physics* 89(7):4001.

Azmi, S. A. M., M. R. Sahar, S. K. Ghoshal, and R. Arifin. 2015. "Modification of structural and physical properties of samarium doped zinc phosphate glasses due to the inclusion of nickel oxide nanoparticles." *Journal of Non-Crystalline Solids* 411:53–58.

Babu, S., M. Seshadri, A. Balakrishna, V. R. Prasad, and Y. C. Ratnakaram. 2015. "Study of multicomponent fluoro-phosphate based glasses: Ho^{3+} as a luminescence center." *Physica B: Condensed Matter* 479:26–34.

Carnall, W. T., P. R. Fields, and K. Rajnak. 1968. "Electronic energy levels in the trivalent lanthanide aquo ions. I. Pr^{3+}, Nd^{3+}, Pm^{3+}, Sm^{3+}, Dy^{3+}, Ho^{3+}, Er^{3+}, and Tm^{3+}." *The Journal of Chemical Physics* 49(10):1785–3797.

Davis, E. A. and N. F. Mott. 1970. "Conduction in non-crystalline systems V. conductivity, optical absorption and photoconductivity in amorphous semiconductors." *Philosophical Magazine* 22(179):0903–22.

Dousti, M.R., S. K. Ghoshal, R. J. Amjad, M. R. Sahar, F. Nawaz, and R. Arifin. 2013. "Structural and optical study of samarium doped lead zinc phosphate glasses." *Optics Communications* 300:204–9.

El-Mallawany, R., M. D. Abdalla, and I. A. Ahmed. 2008. "New tellurite glass: optical properties." *Materials Chemistry and Physics* 109(2–3):291–96.

Ganguli, M., M. H. Bhat, and K. J. Rao. 1999. "Lithium ion transport in Li_2SO_4–Li_2O–P_2O_5 glasses." *Solid State Ionics* 122(February):23–33.

Honma, T., R. Sato, Y. Benino, T. Komatsu, and V. Dimitrov. 2000. "Electronic polarizability, optical basicity and XPS spectra of Sb_2O_3-B_2O_3 glasses." *Journal of Non-Crystalline Solids* 272:1–13.

Hussain, N. S., N. Ali, A. G. Dias, M. A. Lopes, J. D. Santos, and S. Buddhudu. 2006. "Absorption and emission properties of Ho^{3+} doped lead-zinc-borate glasses." *Thin Solid Films* 515(1):318–25.

Jlassi, I., H. Elhouichet, and M. Ferid. 2016. "Influence of MgO on structure and optical properties of alumino-lithium-phosphate glasses." *Physica E: Low-dimensional Systems and Nanostructures* 81:219–25.

Khor, S. F., Z. A. Talib, F. Malek, and E. M. Cheng. 2013. "Optical properties of ultraphosphate glasses containing mixed divalent zinc and magnesium ions." *Optical Materials* 35(3):629–33.

Khor, S. F., Z. A. Talib, and W. M. Mat Yunus. 2012. "Optical properties of ternary zinc magnesium phosphate glasses." *Ceramics International* 38(2):935–40.

Lee, T. H., Y. K. Kwon, and J. Heo. 2008. "Local structure and its effect on the oscillator strengths and emission properties of Ho^{3+} in chalcohalide glasses." *Journal of Non-Crystalline Solids* 354(27):3107–12.

Mahamuda, Sk., K. Swapna, P. Packiyaraj, A. Srinivasa Rao, and G. Vijaya Prakash. 2013. "Visible red, NIR and mid-IR emission studies of Ho^{3+} doped zinc alumino bismuth borate glasses." *Optical Materials* 36(2):362–71.

Mahraz, Z. A. S., M. R. Sahar, and S. K. Ghoshal. 2014. "Band gap and polarizability of boro-tellurite glass: influence of erbium ions." *Journal of Molecular Structure* 1072(1):238–41.

Malinowski, M., M. Kaczkan, A. Wnuk, and M. Szufliñska. 2004. "Emission from the high lying excited states of Ho^{3+} ions in YAP and YAG crystals." *Journal of Luminescence* 106(3–4):269–79.

Mhareb, M. H. A., S. Hashim, S. K. Ghoshal, Y. S. M. Alajerami, M. J. Bqoor, A. I. Hamdan, M. A. Saleh, and M. K. B. Abdul Karim. 2016. "Effect of Dy_2O_3 impurities on the physical, optical and thermoluminescence properties of lithium borate glass." *Journal of Luminescence* 177:366–72.

Nurhafizah, H., M. S. Rohani, and S. K. Ghoshal. 2016. "Er^{3+}:Nd^{3+} concentration dependent spectral features of lithium-niobate-tellurite amorphous media." *Journal of Non-Crystalline Solids* 443:23–32.

Omrani, R. O., A. Kaoutar, A. El Jazouli, S. Krimi, I. Khattech, M. Jemal, J.-J. Videau, and M. Couzi. 2015. "Structural and thermochemical properties of sodium magnesium phosphate glasses." *Journal of Alloys and Compounds* 632:766–71.

Prasad, N. V. V, K. Annapurna, N. S. Hussain, and S. Buddhudu. 2003. "Spectral analysis of Ho^{3+}: TeO_2-B_2O_3-Li_2O glass." *Materials Letters* 57(13–14):2071–80.

Rai, S. and A. L. Fanai. 2016. "Optical properties of Ho^{3+} in sol-gel silica glass Co-doped with aluminium." *Journal of Non-Crystalline Solids* 449:113–18.

Satyanarayana, T., T. Kalpana, V. R. Kumar, and N. Veeraiah. 2010. "Role of Al coordination in barium phosphate glasses on the emission features of Ho^{3+} ion in the visible and IR spectral ranges." *Journal of Luminescence* 130(3):498–506.

Seshadri, M., L. C. Barbosa, and M. Radha. 2014. "Study on structural, optical and gain properties of 1.2 and 2.0 um emission transitions in Ho^{3+} Doped tellurite glasses." *Journal of Non-Crystalline Solids* 406:62–72.

Seshadri, M., Y. C. Ratnakaram, D. T. Naidu, and K. V. Rao. 2010. "Investigation of spectroscopic properties (absorption and emission) of

Ho^{3+} doped alkali, mixed alkali and calcium phosphate glasses." *Optical Materials* 32(4):535–42.

Shannon, R. D. 1976. "Revised Effective Ionic Radii and Systematic Studies of Interatomic Distances in Halides and Chalcogenides." *Acta Crystallographica* A32(32):751–67.

Singh, S. and K. Singh. 2014. "Effect of in-situ reduction of Fe^{3+} on physical, structural and optical properties of calcium sodium silicate glasses and glass ceramics." *Journal of Non-Crystalline Solids* 386:100–104.

Urbach, F. 1953. "The long-wavelength edge of photographic sensitivity and of the electronic absorption of solids " *Physical Review* 92(5):1324.

Venkateswarlu, M. Sk. Mahamuda, K. Swapna, M. V.V. K. S. Prasad, A. S. Rao, S. Shakya, A. M. Babu, and G. V. Prakash. 2015. "Holmium doped lead tungsten tellurite glasses for green luminescent applications." *Journal of Luminescence* 163:64–71.

Vijayakumar, R., G. Venkataiah, and K. Marimuthu. 2015. "Structural and luminescence studies on Dy^{3+} doped boro-phosphate glasses for white LED's and laser applications." *Journal of Alloys and Compounds* 652:234–43.

Wu, F., S. Li, Z. Chang, H. Liu, S. Huang, and Y. Yue. 2016. "Local structure characterization and thermal properties of P_2O_5-MgO-Na_2O-Li_2O glasses doped with SiO_2." *Journal of Molecular Structure* 1118:42–47.

Yusoff, N. M. and M. R. Sahar. 2015. "Effect of silver nanoparticles incorporated with samarium-doped magnesium tellurite glasses." *Physica B: Physics of Condensed Matter* 456:191–96.

Yusoff, N. M., M. R. Sahar, and S. K. Ghoshal. 2015. "Sm3+:Ag NPs assisted modification in absorption features of magnesium tellurite glass." *Journal of Molecular Structure* 1079:167–72.

Zhao, X., X. Wang, H. Lin, and Z. Wang. 2007. "Correlation among Electronic polarizability, optical basicity and interaction parameter of Bi_2O_3-B_2O_3 glasses." *Physica B: Condensed Matter* 390(1–2):293–300.